Neurobiology of Disease

Transient Receptor Potential Canonical 3 (TRPC3) Is Required for IgG Immune Complex-Induced Excitation of the Rat Dorsal Root Ganglion Neurons

Lintao Qu,[1] Yumei Li,[2] Xinghua Pan,[2] Pu Zhang,[1] Robert H. LaMotte,[1] and Chao Ma[1,3]

Departments of [1]Anesthesiology and [2]Genetics, Yale University School of Medicine, New Haven, Connecticut 06510, and [3]Department of Anatomy, Histology and Embryology, Institute of Basic Medical Sciences, Chinese Academy of Medical Sciences, School of Basic Medicine, Peking Union Medical College, Beijing 100005, China

Chronic pain may accompany immune-related disorders with an elevated level of serum IgG immune complex (IgG-IC), but the underlying mechanisms are obscure. We previously demonstrated that IgG-IC directly excited a subpopulation of dorsal root ganglion (DRG) neurons through the neuronal Fc-gamma receptor I (FcγRI). This might be a mechanism linking IgG-IC to pain and hyperalgesia. The purpose of this study was to investigate the signaling pathways and transduction channels activated downstream of IgG-IC and FcγRI. In whole-cell recordings, IgG-IC induced a nonselective cation current (I_{IC}) in the rat DRG neurons, carried by Ca^{2+} and Na^{+}. The I_{IC} was potentiated or attenuated by, respectively, lowering or increasing the intracellular Ca^{2+} buffering capacity, suggesting that this current was regulated by intracellular calcium. Single-cell RT-PCR revealed that transient receptor potential canonical 3 (TRPC3) mRNA was always coexpressed with FcγRI mRNA in the same DRG neuron. Moreover, ruthenium red (a general TRP channel blocker), BTP2 (a general TRPC channel inhibitor), and pyrazole-3 (a selective TRPC3 blocker) each potently inhibited the I_{IC}. Specific knockdown of TRPC3 using small interfering RNA attenuated the IgG-IC-induced Ca^{2+} response and the I_{IC}. Additionally, the I_{IC} was blocked by the tyrosine kinase Syk inhibitor OXSI-2, the phospholipase C (PLC) inhibitor neomycin, and either the inositol triphosphate (IP_3) receptor antagonist 2-aminoethyldiphenylborinate or heparin. These results indicated that the activation of neuronal FcγRI triggers TRPC channels through the Syk–PLC–IP_3 pathway and that TRPC3 is a key molecular target for the excitatory effect of IgG-IC on DRG neurons.

Introduction

Chronic pain is a major health problem that may accompany numerous immune-related diseases (Moulin, 1998; Mathsson et al., 2006; McDougall, 2006; Wittkowski et al., 2007; Oaklander, 2008; Kaida et al., 2009). The IgG immune complex (IgG-IC) appears to be an important factor for the pathogenesis of such pain in addition to the contributions of inflammatory mediators, such as certain chemokines and cytokines (Mathsson et al., 2006; Kaida et al., 2009). IgG-IC produced cutaneous hyperalgesia after the injection of a foreign antigen into the hindpaws of animals immunized with the same antigen and expressing an elevated level of serum IgG (Verri et al., 2008; Ma et al., 2009). However, the neural mechanisms whereby IgG-IC induces pain have not been fully elucidated.

Fc-gamma receptors (FcγRs), the receptors binding to the Fc domain of IgG, are typically expressed in immune cells and have been implicated in the pain generated by inducing the release of proinflammatory cytokines from immune cells (Nimmerjahn and Ravetch, 2006, 2008). The FcγR family consists of two functionally different classes, the activating and the inhibitory receptors. Among them, FcγRI is the only high-affinity activating receptor. Recent studies revealed that FcγRI, but not FcγRII or FcγRIII, is expressed in nociceptive dorsal root ganglion (DRG) neurons (Andoh and Kuraishi, 2004; Qu et al., 2011a). Moreover, neuronal FcγRI appears to be a key player mediating the direct effect of IgG-IC on DRG neurons. The activation of neuronal FcγRI by IgG-IC produced an increase in intracellular calcium ($[Ca^{2+}]_i$) and directly caused the membrane depolarization of DRG neurons (Qu et al., 2011a). However, the ionic mechanisms whereby IgG-IC-evoked activation of FcγRI leads to neuronal excitation remain unknown.

Our recent study (Qu et al., 2011a) showed that the activation of FcγRI by IgG-IC decreased the input resistance and depolarized the membrane potential of the DRG neurons, suggesting that the effect of IgG-IC involves the opening of cation channels. In the human monocytic cell line, FcγRI activation indirectly triggered a nonselective cation channel (NSCC) (Floto et al.,

Received December 20, 2011; revised May 20, 2012; accepted May 23, 2012.

Author contributions: L.Q., R.H.L., and C.M. designed research; L.Q., Y.L., X.P., P.Z., and C.M. performed research; Y.L. and X.P. contributed unpublished reagents/analytic tools; L.Q., Y.L., X.P., P.Z., and C.M. analyzed data; L.Q., R.H.L., and C.M. wrote the paper.

This work was supported by National Institute of Neurological Disorders and Stroke Grants NS065091 (C.M.) and NS014624 (R.H.L.), by a Research Startup Grant (C.M.) from the Department of Anesthesiology, Yale University School of Medicine, by the Peking Union Medical College, Chinese Academy of Medical Sciences, Institute of Basic Medical Sciences Dean's Fund 2011RC01 (C.M.). L.Q. is the recipient of a fellowship from the Canadian Institutes of Health Research. We thank Dr. Sven-Eric Jordt in the Department of Pharmacology, Yale University School of Medicine, for the gift of HC-030031.

The authors declare no competing financial interests.

Correspondence should be addressed to Chao Ma, Department of Anatomy, Histology and Embryology, Institute of Basic Medical Sciences, Chinese Academy of Medical Sciences, School of Basic Medicine, Peking Union Medical College, Beijing 100005, China. E-mail: chao.ma@yale.edu.

DOI:10.1523/JNEUROSCI.6355-11.2012

 0270-6474/12/329554-09$15.00/0

1997). Furthermore, the activity of this channel was enhanced by the depletion of intracellular Ca^{2+} stores independently of FcγRI, suggesting the involvement of a store-operated channel (SOC). However, the molecular identity of this channel is unclear. Transient receptor potential canonical (TRPC) channels (including subtypes 1–7), a family of Ca^{2+}-permeable NSCCs, play a critical role in the regulation of resting membrane potential in excitable cells (Pedersen et al., 2005). All TRPC channels, except TRPC2, are present in rat DRG neurons, with TRPC1, 3, and 6 the most abundant (Kress et al., 2008). Furthermore, some of the TRPCs are activated via a store-operated mechanism (Wu et al., 2010). More recently, TRPC3/6/7 was identified as a key downstream transduction channel in Fc-ε receptor I (FcεRI) signaling in mast cells (Sanchez-Miranda et al., 2010).

Therefore, the present study examined the potential role of TRPC channels in mediating the depolarizing effects of IgG-IC and the associated cellular mechanisms in rat DRG neurons. Preliminary results of this study were presented in abstract form (Qu et al., 2011b).

Materials and Methods

Animals. The adult Sprague Dawley rats (120–180 g) used in this study were all female to maintain consistency with our previous studies (Ma and LaMotte, 2005; Ma et al., 2006). Rats were housed in groups of three or four under a 12 h light/dark cycle. All the experimental procedures were approved by the Institutional Animal Care and Use Committee of Yale University School of Medicine and were conducted in accordance with the guidelines provided by the National Institute of Health and the International Association for the Study of Pain.

Cell dissociation and culture. DRG neurons were cultured from adult Sprague Dawley rats as described previously (Qu et al., 2011a). Briefly, bilateral L4 and L5 lumbar DRGs were harvested from rats and transferred into oxygenated complete saline solution (CSS) for cleaning and mincing. The CSS contained the following (in mM): 137 NaCl, 5.3 KCl, 1 $MgCl_2$, 3 $CaCl_2$, 25 sorbitol, and 10 HEPES, adjusted to pH 7.2 with NaOH. The DRGs were then digested with Liberase TH (0.19 U/ml; Roche Diagnostics) for 20 min and for another 20 min with Liberase TL (0.25 U/ml; Roche Diagnostics) and papain (30 U/ml; Worthington Biochemical) in CSS containing 0.5 mM EDTA at 37°C. After enzymatic digestion, the cells were dissociated by gentle trituration with a fire-polished Pasteur pipette in culture medium containing 1 mg/ml bovine serum albumin and 1 mg/ml trypsin inhibitor (Boehringer Mannheim) and placed on poly-D-lysine/laminin-coated glass coverslips (BioCoat; BD Biosciences). The culture medium contained equal amounts of DMEM and F12 (Invitrogen) with 10% FCS (HyClone Laboratories) and 1% penicillin-streptomycin (Invitrogen). The cells were maintained at 37°C in a humidified atmosphere of 95% air and 5% CO_2 and were used within 24 h.

Preparation of IgG immune complex. IgG-IC was prepared as we previously described (Qu et al., 2011a) using the normal mouse IgG (Santa Cruz Biotechnology) as antigen and the affinity-purified rat anti-mouse IgG (Jackson ImmunoResearch) as antibody. To avoid the possible toxic and nonspecific effects of sodium azide on DRG neurons, the storage buffer of all the IgGs (containing sodium azide) was changed to HEPES buffer using Zeba spin desalting columns (Thermo Scientific) before application. IgG-IC was formed by incubating 10 μg/ml antigen and antibody at the ratio of 1:1 for 1 h at 25°C. Since IgG-IC at the concentration of 0.1 μg/ml displayed the strongest effect on the excitation of DRG neurons in our previous study (Qu et al., 2011a), the concentration of 0.1 μg/ml IgG-IC was used throughout this study.

Calcium imaging. Calcium imaging was performed on cultured rat DRG neurons, as described previously (Qu et al., 2011a). Briefly, DRG neurons were loaded with 2 μM Fura 2-acetoxymethyl ester (Invitrogen) in the dark for 45 min at 37°C and then washed twice in a HEPES buffer containing the following (in mM): 145 NaCl, 3 KCl, 2 $MgCl_2$, 2 $CaCl_2$, 10 glucose, and 10 HEPES, adjusted to pH 7.4 with NaOH. Cells were alternatively excited at 340 and 380 nm using a Polychrome V Monochromator (TILL Photonics). Images were recorded at 2 s intervals at room temperature (20–22°C) using a cooled CCD camera (Sensicam) controlled by a computer with Image Workbench 5.2 software (Indec Biosystems). The ratio of 340 to 380 nm fluorescence intensity [$R_{(340/380)}$] within a certain region of interest after background subtraction was used as a relative measure of intracellular calcium concentration ($[Ca^{2+}]_i$) (Grynkiewicz et al., 1985). Calibration with external standards (Calcium Calibration Buffer Kit; Invitrogen) showed that $R_{(340/380)}$ increased linearly with $[Ca^{2+}]_i$ up to approximately 1 μM and that $R_{(340/380)}$ of 0.7–1.25 corresponded to basal $[Ca^{2+}]_i$ of 90–180 nM. Therefore, only small diameter neurons ($\leq$30 μm) with $R_{(340/380)}$ at the range of 0.7–1.25 were included in this study.

Whole-cell patch-clamp recordings. Whole-cell recordings were performed on small diameter ($\leq$30 μm) DRG neurons with IgG-IC responsiveness identified by calcium imaging. The patch pipettes were pulled from borosilicate glass capillaries (Sutter Instrument; 1.2 mm outer diameter, 0.69 mm inner diameter) using a horizontal puller (model P97; Sutter Instrument). The resistance of the patch pipette was 3–4 MΩ when filled with an internal solution consisting of the following (in mM): 120 K^+-gluconate, 20 KCl, 1 $CaCl_2 \cdot 2H_2O$, 2 $MgCl_2 \cdot 6H_2O$, 11 EGTA, 10 HEPES-K^+, 2 MgATP, with pH adjusted to 7.2 using Tris-base and osmolarity adjusted to 290–300 mOsm with sucrose. Series resistance was routinely compensated at 60–80%. Whole-cell currents were sampled at 20 kHz and filtered at 2 kHz using a Multiclamp 700A amplifier and Pclamp 9 software package (Molecular Devices). Current–voltage (I–V) plots were obtained at a holding potential of −60 mV with 750 ms voltage ramps at an interval of 2 s from −100 to −10 mV (Sun et al., 2006). A neuron was included only if the resting membrane potential was more negative than −40 mV. Since the mean capacitance of the small-size DRG neurons tested in each group was similar (data not shown), the peak amplitude of the currents rather than the current density (the ratio of peak amplitude to cell capacitance) was measured in this study for comparisons between groups. The neuron was considered capsaicin sensitive if an inward current was induced by the puff application of capsaicin (1 μM) for 10 s at the end of whole-cell recordings. All the experiments were performed at room temperature (20–22°C).

The DRG neurons were continuously perfused with the HEPES buffer. In some experiments, the Ca^{2+}-free bath solution was applied in which the normal bath solution (HEPES buffer) was modified by the removal of 2 mM $CaCl_2$, the addition of 0.1 mM EGTA, and an increase in the concentration of $MgCl_2$ (4 mM) (Lu et al., 2006). The Na^+-free bath solution was the same as the normal HEPES buffer, except that extracellular Na^+ was replaced by *N*-methyl-D-glucamine (NMDG). For delineation of Ca^{2+} permeability, the bath solution with Ca^{2+} as the sole cationic charge carrier (Ca^{2+}-only solution) was used as previously described (Poteser et al., 2011) and contained the following (in mM): 135 NMDG, 3 $CaCl_2$, 7 Ca-gluconate, 2 $MgCl_2$, 10 glucose, and 10 HEPES, at pH adjusted to 7.4 with methanesulfonic acid. The internal solutions with high and low Ca^{2+} buffer capacity were obtained by replacing 11 mM EGTA with 10 mM BAPTA and decreasing the concentration of Ca^{2+} and EGTA in the normal internal solution to 0.5 and 1 mM, respectively (Qiu et al., 2010). All agents were dissolved in HEPES buffer and applied locally to the neuronal cell bodies through a micropipette with a tip diameter of 100 μm and an 8-channel, pressure-controlled drug application system (AutoMate Scientific) (Ma et al., 2006). The interval between drug applications was 5–6 min. All chemicals were purchased from Sigma-Aldrich unless otherwise indicated.

Single-cell reverse-transcription PCR. The individual small-size DRG neurons were first examined for IgG-IC sensitivity by calcium imaging and then aspirated into a glass electrode with a tip diameter of 25–40 μm and gently transferred into a PCR tube. For the negative control, a sample of the bath solution without any cell contents was used. The total RNA was extracted from individual DRG neuron using an RNeasy Plus Micro kit (Qiagen). The RNA was reverse transcribed using Superscript Reverse Transcriptase II (Invitrogen) according to the manufacturer's instructions. PCR amplification was then performed using a Titanium TaqPCR Kit (Clontech) with the primers as shown in Table 1. Beta III-tubulin was used as an internal control. The temperature cycles included an initial 4-min denaturing step at 94°C followed by 40 cycles of 30 s denaturation

Table 1. List of DNA primer sequences designed for single-cell RT-PCR

Target gene	Primer sequence 5′-3′	Product length (bp)	GenBank no.
CD64	AGTTGGAGCTATTTGGTCCCCAGTC GCTAAGGTCCAGGGTCACCTGA	300	NM_001100836.1
TRPC1	AGACGGCAGAACAGCTTGAAGGAGT CACGGTGGCTTGGTCTGTGCTC	141	NM_053558.1
TRPC3	TGATGAGGTGAACGAAGGTGAACTG TGCCCACATTTGTGCCAGAGTCA	206	NM_021771.2
TRPC4	AATTACTCGTCAACAGGCGGC CACCACCACCTTCTCCGACTT	203	NM_080396.1
TRPC5	AAGTTTCGAATTTGAGGAGCAGATG AATCTCTGATGGCATCGCACA	220	NM_080898.2
TRPC6	GCTCATCCAAACTGTCAGCA CAGCATTCCAAAGTCAAGCA	216	NM_053559.1
TRPC7	ATGACGAGTTCTATGCCTACGACG TTGTAGGCATTCATACGGGAGC	226	NM_001191691.2
β3-tubulin	GTCCGCCTGCCTCTTCGTCTC TTGCCAGCACCACTCTGACCGAA	335	NM_139254.2

at 94°C, 30 s annealing at 58°C, and 30 s elongation at 68°C. The reaction was completed with 5 min of final elongation at 68°C. The PCR products were displayed on an ethidium bromide-stained 2% agarose gel.

Small interfering RNA transfection. DRG neurons were transfected with either a Stealth small interfering RNA (siRNA) or a Stealth RNAi negative control (Invitrogen) using the Lipofectamine 2000 transfection reagents (Invitrogen) according to the manufacturer's instructions. The target sequences of the Stealth siRNAs were 5′ CCA CCC AGU UCA CAU GGA CAG AAA U 3′ and 5′ AUU UCU GUC CAU GUG AAC UGG GUG G 3′ for TRPC3; and 5′ CCA UGA CCA CUG GUA GAC AAC CAA U 3′ and 5′ AUU GGU UGU CUA CCA GUG GUC AUG G 3′ for the scrambled control of TRPC3 (Shirakawa et al., 2010). After 6 h treatment with siRNA, the medium was changed with DMEM containing 10% FCS, and the cells were incubated for 24–36 h. The neurons without the addition of siRNA to the transfection reagents were used as an empty vector negative control.

Quantitative RT-PCR analysis. Total RNA was extracted from DRG neurons 48 h after transfection with scrambled or TRPC3 siRNA and then were reverse transcribed as described above. Following cDNA synthesis, qRT-PCR was performed using an iCycler single-color real-time PCR detection system (Bio-Rad) with iQ SYBR Green Supermix (Bio-Rad). The sequences of primers for TRPC3 and β3-tubulin control are presented in Table 1. The qPCR condition was 94°C for 4 min, followed by 40 cycles of 94°C for 30 s, 58°C for 25 s, and 72°C for 20 s. After 5 min of final extension at 72°C, a melt curve was generated. The identity of the PCR products was confirmed by automated determination of the melting temperature of the PCR products. The amplicons were displayed on an ethidium bromide-stained 2% agarose gel.

Immunofluorescent staining. Immunofluorescent labeling was performed on the dissociated rat DRG neurons to evaluate the expression level of TRPC3 receptors in DRG neurons under control and siRNA-treated conditions. Briefly, neurons were fixed by 2% paraformaldehyde for 20 min and incubated with blocking buffer (10% normal horse serum and 0.2% Triton X-100 (Sigma-Aldrich) in PBS) for 1 h, followed by incubation with the primary antibody (rabbit-anti-TRPC3, 1:400; Alomone Labs) at room temperature for 1 h and then with the secondary antibodies (Alexa Fluor 488-conjugated donkey-anti-rabbit, 1:500; Invitrogen) for 1 h. Control staining was performed without primary antibody. The neurons were then washed in PBS and coverslipped with ProLong Gold antifade reagent with DAPI (Invitrogen) to stain nuclear profiles. The cells were visualized and the images were captured using a laser confocal microscopic imaging system (LMS 510; Carl Zeiss MicroImaging). The number of immunofluorescence-positive cells was counted using ImagePro Plus 5.0 (Media Cybernetics).

Data analysis. Data values are presented as mean ± SEM. For a series of experiments in which IgG-IC was applied twice in normal conditions or under several chemical treatments, the second peak amplitude of currents induced by IgG-IC was expressed as the percentage of the first response. Statistical analyses were performed using the SPSS 18.0 software (IBM). A Student's *t* test was used for comparisons between two groups. Comparisons for more than three groups were carried out using

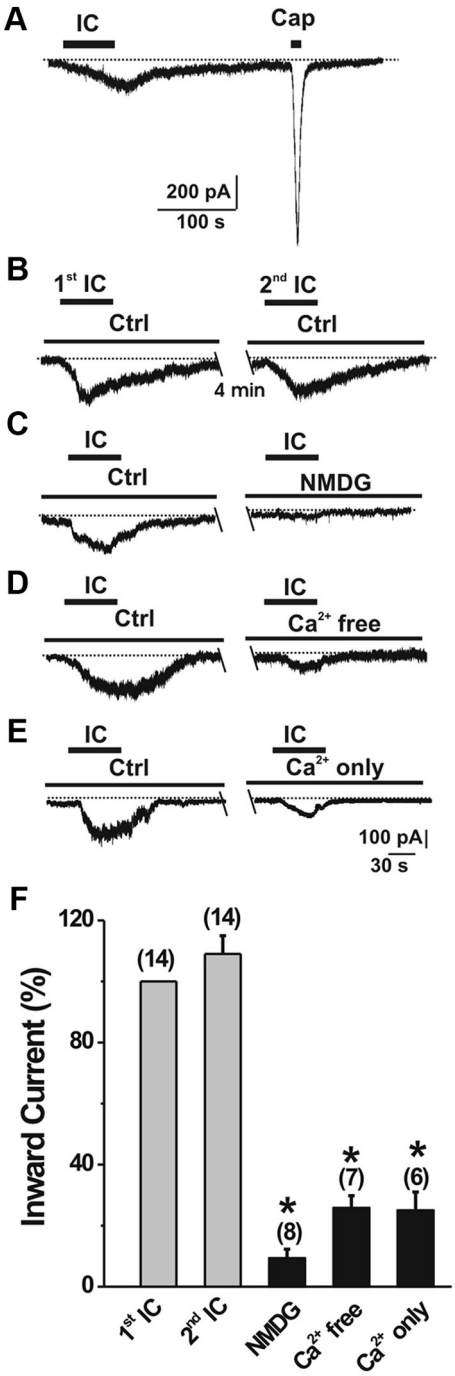

Figure 1. IgG-IC induced a cation current in small-size DRG neurons. The neurons were held at −60 mV in voltage-clamp mode. ***A***, Typical traces of inward currents evoked by IgG-IC (0.1 μg/ml; 1 min) and capsaicin (1 μM; 10 s). ***B***–***E***, Representative traces of I_{IC} in a control HEPES bath solution (***B***), an NMDG solution (***C***), a Ca^{2+}-free bath solution (***D***), or a bath solution containing Ca^{2+} (10 mM) as the only cation (***E***). ***F***, Summary of contributions of extracellular Na^{+} and Ca^{2+} to the I_{IC}. Replacement of extracellular Na^{+} or Ca^{2+} significantly attenuated the I_{IC}. I_{IC} was decreased after switching to bath solution containing Ca^{2+} as the major cation. As a control, sequential application of IgG-IC at an interval of 5–6 min induced inward currents with the similar peak amplitudes. For each group, the first peak of the I_{IC} in control HEPES bath solution was normalized as 100%. *$p < 0.001$ versus second IC. The number of cells tested is indicated in parentheses.

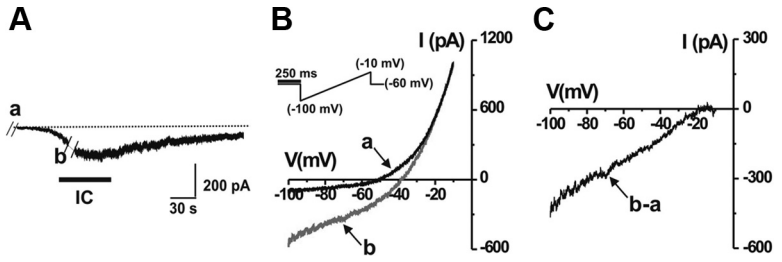

Figure 2. *I–V* relationship of the I_{IC}. ***A***, Application of IgG-IC (0.1 μg/ml; 1 min) induced an inward current at a holding potential of −60 mV. ***B***, Voltage ramps from −100 mV to −10 mV with a duration of 750 ms (inset) were applied every 2 s before (a) and during (b) the application of IgG-IC (0.1 μg/ml). ***C***, *I–V* relationship of the I_{IC} was obtained by subtracting a from b. The I_{IC} reversed near −15 mV for the sample cell.

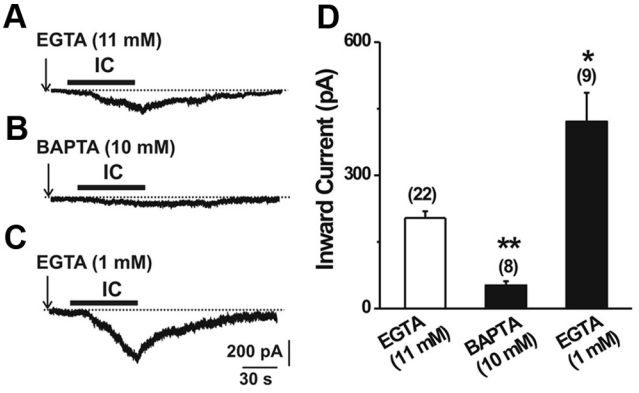

Figure 3. The I_{IC} was modulated by $[Ca^{2+}]_i$. ***A–C***, Typical traces of the I_{IC} recorded at a holding potential of −60 mV using the internal solution containing 11 mM EGTA (***A***), 10 mM BAPTA (***B***), or 1 mM EGTA (***C***). ***D***, Decreasing $[Ca^{2+}]_i$ with fast Ca^{2+} chelator BAPTA (10 mM) significantly attenuated the I_{IC} whereas lowering the Ca^{2+} buffer capacity dramatically enhanced this current. Numbers in parentheses indicate the number of cells tested. *$p < 0.05$ and **$p < 0.001$ versus 11 mM EGTA.

one-way ANOVA followed by Scheffé's *post hoc* test. Comparisons of proportions were made using the χ^2 test. Differences were considered statistically significant if $p < 0.05$.

Results

IgG immune complex induces a nonselective cationic channel current

To determine the ionic mechanisms underlying the IgG-IC-induced depolarization, whole-cell voltage clamp recordings were performed on cultured DRG neurons before and after IgG-IC application. Bath application of IgG-IC (0.1 μg/ml) for 1 min induced an inward current (I_{IC}) with a peak amplitude of 204.2 ± 15.2 pA ($n = 22$) when the neurons were held at −60 mV (Fig. 1*A*). The I_{IC} returned slowly to baseline within 3 min after washout of IgG-IC in all the neurons tested. Moreover, 72% of these neurons showed an inward current evoked by capsaicin (1 μM; Fig. 1*A*). When IgG-IC (0.1 μg/ml) was applied twice at an interval of 5–6 min, the peak of the second I_{IC} was 193.8 ± 19.1 pA, which was not significantly different from the 206.8 ± 24.6 pA of the first (Fig. 1*B*,*F*; $n = 14$; $p > 0.05$), suggesting that no desensitization occurred during repetitive applications of IgG-IC at the concentration of 0.1 μg/ml.

To examine the contributions of extracellular Na^+ or Ca^{2+} to the I_{IC}, Na^+ and Ca^{2+} were, respectively, separately removed from the HEPES buffer. When extracellular Na^+ was replaced by NMDG, a large organic cation that cannot pass through cationic channels, the I_{IC} was decreased nearly to the baseline ($n = 7$) (Fig. 1*C*,*F*). Removal of extracellular Ca^{2+} significantly reduced the peak amplitude of the I_{IC} ($n = 8$) (Fig. 1*D*,*F*), suggesting the Ca^{2+} dependence of the I_{IC}. In addition, switching the normal bath solution (2 mM Ca^{2+}) to the solution containing Ca^{2+} (10 mM) as the sole cation ($n = 6$) (Fig. 1*E*,*F*), abolished most, but not all, of the I_{IC}, indicating that the I_{IC} is only partially carried by Ca^{2+}. Therefore, the I_{IC} appears to be mediated by an NSCC, which is more likely carried by Na^+ and Ca^{2+}.

To further estimate the *I–V* relationship of the I_{IC}, a voltage ramp from −100 mV to −10 mV with a slope of 120 mV/s (Sun et al., 2006) was applied before and during IgG-IC application (Fig. 2*A*,*B*, inset), and the responding membrane current was recorded. The I_{IC} for each neuron was obtained by subtracting the membrane current recorded in the absence of IgG-IC from that recorded in the presence of IgG-IC (Fig. 2*C*). To rule out the possible contaminations of action potentials, the membrane potential was only depolarized from −100 mV to −10 mV (Sun et al., 2006). Under physiological ionic conditions of 145 mM Na^+ externally and 140 mM K^+ in the internal solution, the *I–V* relationship of the I_{IC} for each neuron tested was linear over the voltage ranges tested, indicating a lack of voltage dependency (Fig. 2*C*). In addition, the mean reversal potential of the I_{IC} was −14.6 ± 2.8 mV ($n = 10$) under physiological ionic conditions.

The I_{IC} is regulated by intracellular calcium

Since the $[Ca^{2+}]_i$ was shown to increase after FcγRI cross-linking in DRG neurons (Andoh and Kuraishi, 2004; Qu et al., 2011a), we next examined whether the I_{IC} is modulated by intracellular calcium. BAPTA, the fast Ca^{2+} chelator, buffers Ca^{2+} ions ~200-fold more rapidly, though BAPTA and EGTA have similar K_Ds for Ca^{2+} binding. Thus, BAPTA chelates $[Ca^{2+}]_i$ more effectively at the same time and spatial scales near Ca^{2+} entry points (Naraghi, 1997; Neher, 1998). When 11 mM EGTA in the internal solution was replaced with 10 mM BAPTA, the peak of the I_{IC} was significantly decreased from 204.2 ± 15.2 pA ($n = 22$) (Fig. 3*A*) in EGTA-buffered internal solution to 53.1 ± 9.5 pA ($n = 8$) (Fig. 3*B*,*D*). By contrast, when intracellular Ca^{2+} buffering capacity was lowered by reducing the concentration of EGTA from 11 to 1 mM in the internal solution, the I_{IC} was dramatically increased to 420.8.± 65.2 pA ($n = 9$) (Fig. 3*C*,*D*), suggesting that the I_{IC} is regulated or sensitized by $[Ca^{2+}]_i$.

TRPC channels contribute to the I_{IC}

When considering a potential molecular target for the IgG-IC, we realized that all the properties of the I_{IC} resembled the TRPC current, one major type of Ca^{2+}-permeable NSCCs. These included nonselectivity for cations, lack of voltage gating, and intracellular Ca^{2+} dependence (Clapham et al., 2005). More important, a recent study revealed that TRPC3/6/7 channel subtypes were involved in IgE-IC-triggered signaling in mast cells (Sanchez-Miranda et al., 2010). Therefore, we tested whether the I_{IC} was mediated by TRPC channels in DRG neurons. To test this possibility, single-cell RT-PCR (scRT-PCR) analysis was used to determine the coexpression pattern of FcγRI (CD64) and TRPC channel subtypes in individual DRG neurons with IgG-IC responsiveness established by calcium imaging. Since TRPC2 is not expressed in rat DRG neurons (Kress et al., 2008), it was excluded from the present study. Consistent with previous studies (Kress et

al., 2008), TRPC5 and TRPC7 were not detected in DRG neurons after 1 d in culture. Among all the neurons tested, the FcγRI-positive population also expressed TRPC3 ($n = 10$) (Fig. 4*A*). In contrast, the coexpression of FcγRI with other TRPC subtypes was not observed consistently across the neurons tested (Fig. 4*A*). These results provide additional evidence that TRPC3 is likely a molecular candidate for the nature of the I_{IC}. Therefore, we next asked whether the I_{IC} is attenuated by pharmacological or genetic knockdown of TRPC3 channels. Bath application of ruthenium red (10 μM), an inhibitor of several TRP channels (Clapham et al., 2005), almost completely blocked the I_{IC} ($n = 7$) (Fig. 4*B*,*F*). When the neurons were pretreated with 10 μM BTP2, a known general TRPC blocker at this dose in native cells (Miyano et al., 2010), the I_{IC} was also significantly attenuated ($n = 7$) (Fig. 4*C*,*F*). Furthermore, pyrazole-3 (10 μM), a selective TRPC3 antagonist (Kiyonaka et al., 2009; Shirakawa et al., 2010), significantly reduced the peak amplitude of the I_{IC} ($n = 7$) (Fig. 4*D*,*F*). Since TRPA1 is also a Ca^{2+}-modulated NSCC (Doerner et al., 2007), we next tested whether TRPA1 contributes to the I_{IC}. Treatment with a selective TRPA1 antagonist, HC-030031 (100 μM), had no significant effect on the I_{IC} ($n = 5$) (Fig. 4*E*,*F*).

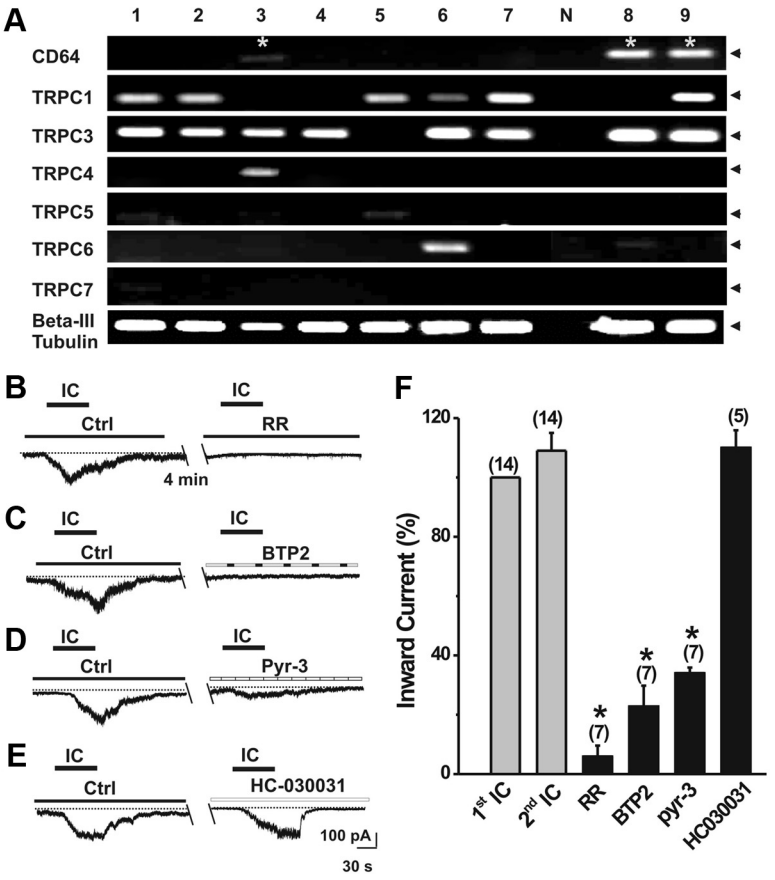

Figure 4. TRPC3 was required for the I_{IC} in small DRG neurons. ***A***, scRT-PCR was performed on individual DRG neurons with the responsiveness to IgG-IC (0.1 μg/ml) established by calcium imaging. FcγRI (CD64) was always colocalized with TRPC3 but not with other TRPC channel subtypes in the same neurons. N, Negative controls from the pipettes that were submerged in the bath solution without harvesting any cell contents. Asterisk indicates the FcγRI (CD64)-positive neurons. Arrowhead indicates the level of individual gene gel band. ***B–E***, Representative traces of the I_{IC} in the presence of a general TRP channel blocker ruthenium red (RR; 10 μM; ***B***), a general TRPC channel blocker BTP2 (10 μM, ***C***), a selective TRPC3 antagonist pyrozole-3 (pyr-3; 10 μM; ***D***), and TRPA1 antagonist HC030031 (100 μM; ***E***). The neuron was held at −60 mV. ***F***, Summary of the effects of TRPC channel blockers on the I_{IC}. Treatment with RR, BTP2, and pyr-3 significantly attenuated the I_{IC} whereas HC030031 had no effect on this current. For each group, the second peak amplitude of the I_{IC} was expressed as the percentage of the first response. $^*p < 0.001$ versus second IC. The number of cells tested is indicated in parentheses.

To further probe the role of TRPC3 in the I_{IC}, TRPC3 was knocked down with a specific siRNA in DRG neurons. The significant reduction of mRNA and protein expression of TRPC3 after siRNA transfection was confirmed by both RT-PCR (Fig. 5*A*) and immunofluorescence staining (Fig. 5*B*), respectively. The expression of TRPC3 was similar in both vector-negative control and scrambled siRNA control. The percentage of TRPC3-immunopositive neurons was significantly lower in the siRNA-treated samples (13.7%, or 20/146) as compared to those treated with scrambled siRNA (43.6%, or 51/117) ($p < 0.001$, χ^2 test). Calcium imaging indicated that IgG-IC-evoked Ca^{2+} responses were significantly suppressed in TRPC3 siRNA-transfected cells ($n = 18$), whereas transfection of a scrambled siRNA ($n = 18$) did not substantially change the IgG-IC effect, as compared to the vector control (Fig. 5*C–E*). In addition, specific knockdown of TRPC3 ($n = 11$) significantly attenuated the peak amplitude of the I_{IC}, whereas the scrambled siRNA ($n = 10$) had no such effect (Fig. 5*F–H*). These findings indicate that TRPC3 is a likely key candidate channel responsible for mediating the I_{IC}.

FcγRI couples to TRPC3 through the spleen tyrosine kinase–phospholipase C–inositol trisphosphate signaling pathway

Activation of FcγRI by IgG-IC is known to stimulate the spleen tyrosine kinase (Syk)–phospholipase C (PLC)–inositol trisphosphate (IP_3) signaling pathway in macrophages and monocytic cell lines (van de Winkel et al., 1990; Liao et al., 1992; Kiener et al., 1993; Bonilla et al., 2000; Nimmerjahn and Ravetch, 2007). Moreover, TRPC channels are activated or modulated by PLC-coupled receptors (Montell, 2008), making them likely downstream targets of IgG-IC. Thus, we next examined whether FcγRI can couple to TRPC channels through the Syk–PLC–IP_3 signaling pathway. Pretreatment with Syk inhibitor OXSI-2 (10 μM; $n = 9$) (Fig. 6*A*,*E*) or PLC inhibitor neomycin (100 μM; $n = 11$) for 4 min almost abolished the I_{IC} ($n = 9$) (Fig. 6*B*,*E*), suggesting that the I_{IC} was mediated through Syk and PLC. TRPC3 was shown to be directly activated by diacylglycerol (DAG) (Zitt et al., 1997; Trebak et al., 2003b). However, the I_{IC} was unlikely to be mediated by DAG since the membrane-permeable DAG analog OAG (100 μM) alone failed to induce an inward current in all IgG-IC responsive neurons tested ($n = 5$) (Fig. 6*C*,*E*). In addition to DAG, TRPC3 channels can interact with IP_3 receptors or can be activated through Ca^{2+} release from internal stores (Kiselyov et al., 1998; Ma et al., 2000). When the neurons was perfused with membrane-permeate IP_3 receptor antagonist 2-APB (100 μM) (Ma et al., 2000; Qiu et al., 2010), the I_{IC} was significantly reduced ($n = 8$) (Fig. 6*D*,*E*). Although 2-APB is also considered as a potent blocker of TRPC channels, it acts on extracellular but not intracellular sites of TRPC channels (Trebak et al., 2002; Xu et al., 2005; Raybould et al., 2007). Thus, to further determine whether

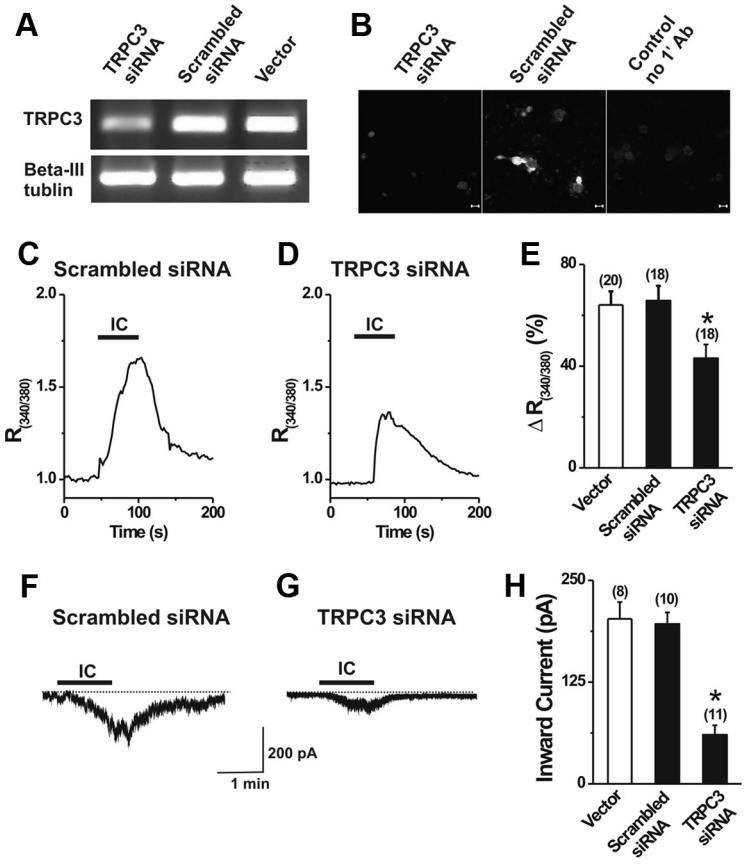

Figure 5. ***A***, ***B***, Knockdown of TRPC3 with a specific siRNA reduced the IgG-IC-induced response. RT-PCR (***A***) and immunofluorescent staining (***B***) showed that TRPC3 siRNA but not scrambled siRNA knocked down the expression of TRPC3 in DRG neurons. The control staining of TRPC3 (***B***, right) was performed without primary antibody (1′ Ab). ***C***, ***D***, Representative Ca^{2+} responses induced by IgG-IC in DRG neurons transfected with a scrambled siRNA (***C***) or TRPC3 siRNA (***D***). ***E***, IgG-IC-induced Ca^{2+} response [$R_{(340/380)}$] was significantly decreased in TRPC3 siRNA-transfected cells, as compared to vector or scrambled siRNA-transfected cells. There were significant differences in IgG-IC-induced Ca^{2+} responses between vector and scrambled siRNA-transfected cells. $^*p < 0.05$ versus vector or scrambled siRNA. ***F***, ***G***, Typical traces of The I_{IC} recorded from DRG neurons transfected with scrambled siRNA (***F***) and TRPC3 siRNA (***G***), respectively. ***H***, The I_{IC} was significantly attenuated by the knockdown of TRPC3 with a specific siRNA whereas the scrambled siRNA had no effect on this current. The neurons were held at −60 mV. $^*p < 0.001$ versus vector or scrambled siRNA. Cell numbers are indicated in parentheses.

the inhibitory effect of 2-APB on the I_{IC} was attributable to a direct blockade of TRPC channels or IP_3 receptors, 2-APB (100 μM) was added to the internal solution. Intracellular 2-APB still produced suppression of the I_{IC} (33.8 ± 6.9 pA, $n = 9$) (Fig. 6*F*,*H*), similar to that when 2-APB was applied to the bath solution (28.5 ± 7.5 pA, $n = 8$). The result suggests that 2-APB mainly acts on IP_3 receptors to block the IgG-IC response. Similarly, the I_{IC} was also inhibited ($n = 6$) (Fig. 6*G*,*H*) when another IP_3 receptor antagonist, heparin (100 μg/ml) (Li et al., 1999), was dialyzed into the cells. Thus, the I_{IC} might be activated through a store-operated mechanism.

Discussion

In this study, we have demonstrated for the first time that IgG-IC elicits a nonselective cation current in DRG neurons via neuronal FcγRI. Moreover, TRPC3 appears to be a key downstream transduction channel mediating the I_{IC}. In addition, the Syk– PLC–IP_3 signaling pathway is likely required for coupling FcγRI to TRPC3 in DRG neurons.

TRPC3 contributes to the I_{IC} in DRG neurons

Our present study provided three lines of original evidence to support the hypothesis that IgG-IC induced a cation current mainly flowing through TRPC3 channels in DRG neurons, therefore contributing to IgG-IC-induced neuronal excitation. First, bath application of IgG-IC elicited an NSCC, which was carried by Na^+ and Ca^{2+} with a reversal potential of approximately −15 mV under physiological conditions. Moreover, the I_{IC} was regulated or sensitized by intracellular Ca^{2+}. These features of the I_{IC} are similar to those of TRPC3 channels *in vitro* (Wu et al., 2010). Accordingly, a recent study revealed that TRPC3/6/7 channel subtypes were involved in FcεRI signaling in mast cells (Sanchez-Miranda et al., 2010). Thus, it is likely that TRPC channels are a potential downstream target of the IgG-IC in the DRG neurons. Second, scRT-PCR results demonstrated a consistent coexpression of FcγRI (CD64) with TRPC3 mRNA in the same DRG neurons, suggesting that FcγRI is more likely associated with the TRPC3, either directly or indirectly. Third, the I_{IC} was blocked by the general TRPC channel inhibitors RR and BTP2 and by the selective TRPC3 antagonist pyrazole-3. Particularly, a knockdown of TRPC3 significantly decreased the I_{IC} and IgG-IC-induced $[Ca^{2+}]_i$ elevations.

We showed that the IgG-IC-induced Ca^{2+} response was less suppressed after transfection of TRPC3 siRNA, as compared to the peak of I_{IC} (35% vs 69%), perhaps because Ca^{2+} release from internal stores is a major source for IgG-IC-induced Ca^{2+} response, in addition to the Ca^{2+} entry from extracellular space, such as through TRPC3 (Qu et al., 2011a). By contrast, the I_{IC} is likely to be mainly mediated by TRPC3 channels. However, a small residual I_{IC} was still detected after pharmacological inhibition or gene knockdown of TRPC3 channels, which might indicate a contribution of other channels, especially in different neuronal types. Among the candidate NSCCs, TRPA1 is highly expressed in DRG neurons and may also function as a Ca^{2+}-gated NSCC (Doerner et al., 2007). However, the TRPA1-selective antagonist HC030031 did not affect the peak of the I_{IC}, suggesting that TRPA1 does not contribute to the I_{IC} in these DRG neurons. In addition, it is unlikely that the I_{IC} is mediated by TRPV1 for the following reasons: first, the I_{IC} can still be observed in a subset of capsaicin-insensitive neurons although the majority of IgG-IC responsive neurons (72%) are sensitive to capsaicin; second, TRPV1 is normally activated by 2-APB (Hu et al., 2004; Colton and Zhu, 2007) whereas the I_{IC} was blocked by 2-APB.

A potential discrepancy between the characteristics of the I_{IC} and the TRPC3 current in expressing cell lines (Zitt et al., 1997; Poteser et al., 2011) is the lack of outward rectification in the I_{IC} recorded in DRG neurons. This difference is likely due to a relatively narrow voltage range (−100 to −10 mV, to avoid action potential contamination) used in this study. It is also possible that the *I–V* relationship of TRPC3 in native cells is different from that in the expressing cell lines (Li et al., 1999). The endogenous I_{IC} in

DRG neurons is only partially carried by Ca^{2+}, which is slightly different from the characteristics of TRPC3 in expressing cell lines while consistent with that in pontine neurons (Li et al., 1999).

Syk–PLC–IP_3 signaling pathway is required for FcγRI coupling to TRPC3

Another important finding of this study is that FcγRI and TRPC3 are functionally coupled to each other through the Syk–PLC–IP_3 signaling pathway. In immune cells, the activation of FcγRI by IgG-IC results in the phosphorylation of Syk, a non-receptor tyrosine kinase (Kiener et al., 1993; Indik et al., 1995). Activated Syk stimulates PLC, which hydrolyzes the membrane phospholipid phosphatidylinositol 4,5-bisphosphate to produce IP_3 and DAG (van de Winkel et al., 1990; Liao et al., 1992; Kiener et al., 1993; Bonilla et al., 2000; Nimmerjahn and Ravetch, 2007). In addition, TRPC3 has been shown to be activated or modulated by PLC signaling (Montell, 2008). Thus, it is likely that FcγRI couples to TRPC3 through the Syk–PLC–IP_3 signaling pathway following IgG-IC treatment. Consistent with this hypothesis, we found, by use of pharmacological inhibitors, that the I_{IC} observed in DRG neurons is mediated by an intracellular signaling pathway involving Syk, PLC, and the IP_3 receptors. We showed that bath application of OXSI-2, the potent Syk inhibitor (Lai et al., 2003), inhibited the I_{IC}. Since the PLC blocker U7322 itself was shown to cause an irreversible increase in $[Ca^{2+}]_i$ in DRG neurons, neomycin was used in this study instead (Bonnington and McNaughton, 2003). The I_{IC} was also blocked by neomycin. In addition, the inclusion of 2-APB or heparin to the pipette solution produced suppression of the I_{IC}. Furthermore, the blocking effects of 2-APB were more likely due to the intracellular blockade of the IP_3 receptors rather than the direct inhibition of TRPC channels since the binding site of 2-APB is normally located extracellularly for the inhibition of TRPC channels (Trebak et al., 2002; Xu et al., 2005; Raybould et al., 2007).

In most of the early studies using TRPC3-expressing cell lines, TRPC3 has been proposed to function as a receptor-operated cation channel that can be activated by DAG but not through the production of IP_3 or via a store-operated mechanism (Hofmann et al., 1999; Trebak et al., 2003a). However, some studies indicated that TRPC3 behaves as an SOC that interacts with IP_3 receptors and is activated through the release of Ca^{2+} from

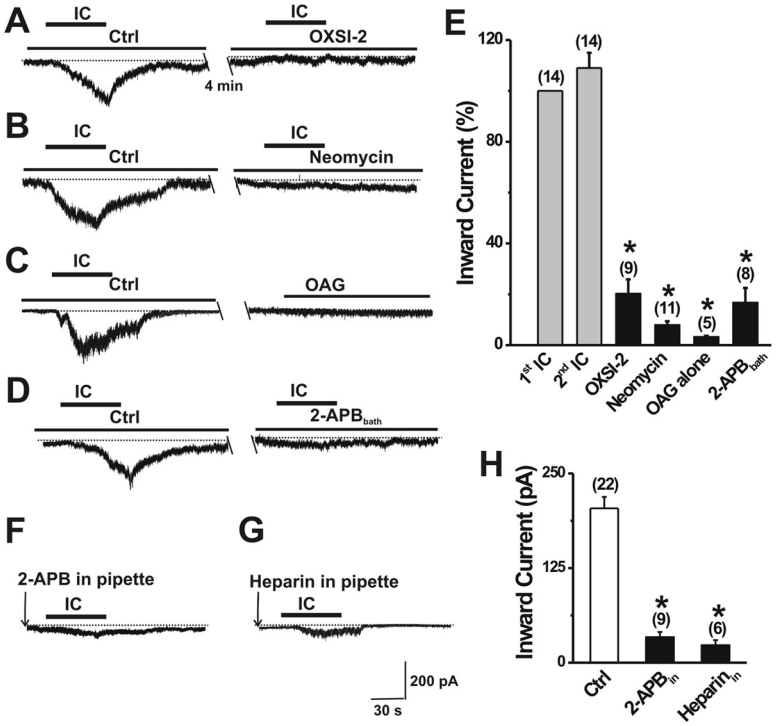

Figure 6. The Syk–PLC–IP_3 signaling pathway was required for functional coupling of FcγRI to TRPC3. ***A–D***, Typical traces of the I_{IC} recorded at a holding potential of −60 mV in the presence of Syk inhibitor OXSI-2 (10 μM; ***A***), PLC inhibitor neomycin (10 μM; ***B***), DAG analog OAG alone (100 μM; ***C***), or IP_3 receptor blocker 2-APB (100 μM; ***D***). ***E***, Treatment with OXSI-2, neomycin and 2-APB substantially reduced the peak amplitude of the I_{IC}. Bath application of OAG alone failed to induce an inward current in IgG-IC-responsive neurons. For each group, the second peak amplitude of the I_{IC} was expressed as the percentage of the first response. $^*p < 0.001$ versus second IC. ***F***, ***G***, Inclusion of 2-APB (100 μM; ***F***) or heparin (100 μg/ml; ***G***) in the patch pipette prevented the I_{IC}. ***H***, Summary of the inhibitory effects of internal 2-APB and heparin on the I_{IC}. $^*p < 0.001$ versus control. The number of cells tested is shown above each bar.

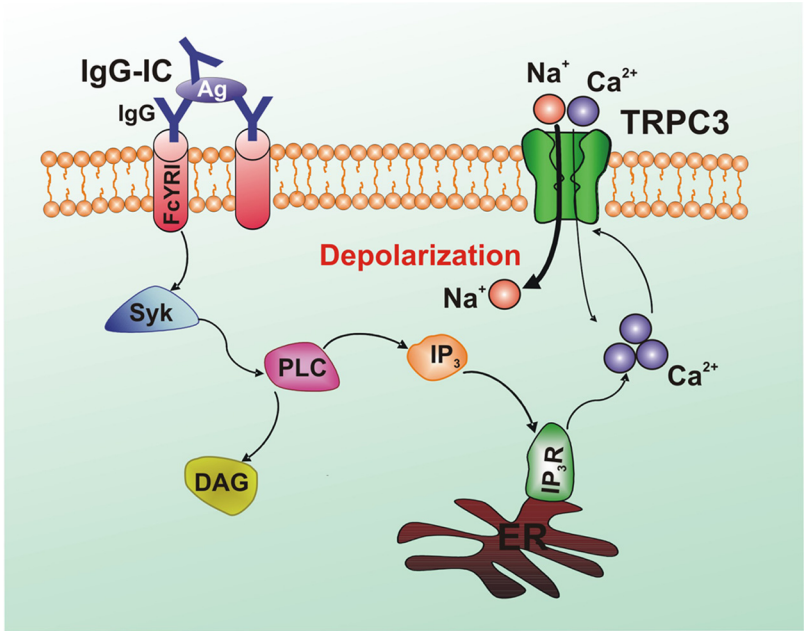

Figure 7. Schematic illustration demonstrating signaling pathways involved in IgG-IC-induced excitation in rat DRG neurons. IgG-IC binding to its receptor (FcγRI) stimulates Syk, which leads to the activation of PLC. PLC subsequently hydrolyzes the phosphatidylinositol 4,5-bisphosphate to generate DAG and IP_3. IP_3 binds to IP_3 receptors in endoplasmic reticulum to induce Ca^{2+} release from internal stores, which in turn enhances or sensitizes TRPC3 activity, resulting in further Ca^{2+} influx and membrane depolarization. However, DAG is unlikely involved in FcγRI-trigged signaling. All these signaling events consequently increase the excitability of DRG neurons.

internal stores (Kiselyov et al., 1998; Ma et al., 2000; Kaznacheyeva et al., 2007; Kim et al., 2009). Here we showed that the I_{IC} was blocked by the IP_3 receptor antagonist 2-APB and heparin and by the SOC blocker BTP2 but was not affected by the DAG analog OAG, indicating that the I_{IC} is more likely activated through a store-operated mechanism in the same way as TRPC3 (Ma et al., 2000; He et al., 2005), consistent with a previous study (Floto et al., 1997). We also showed that lowering the intracellular calcium buffering power potentiated, whereas enhancing the calcium buffering capacity of the internal solution attenuated, the I_{IC}, suggesting that I_{IC} is modulated by $[Ca^{2+}]_i$. Taken together, these findings indicate that IgG-IC activates TRPC3 in DRG neurons through a signaling pathway that involves Syk, PLC, IP_3 receptor, and intracellular Ca^{2+} (Fig. 7). These results suggest that TRPC3 likely behaves as an SOC in FcγRI-triggered signaling in DRG neurons.

Functional implications

IgG-IC plays a critical role in the pathogenesis of pain (Verri et al., 2008; Ma et al., 2009). A predominant immune cell-centric view is that IgG-IC may induce pain and hyperalgesia via the activation of certain immune cells and the release of proinflammatory cytokines (Verri et al., 2007, 2008; Pinto et al., 2010). Moreover, FcγRs, expressed on immune cells, appear to play an important role in this process (Nimmerjahn and Ravetch, 2006, 2008). However, recent studies revealed that IgG-IC directly excited primary sensory neurons though neuronal FcγRI (Andoh and Kuraishi, 2004; Qu et al., 2011a), which may cause pain sensation. In addition, activation of neuronal FcγRI triggered the release of certain proinflammatory neurotransmitters from DRG neurons, such as substance P (Andoh and Kuraishi, 2004). These mediators may further induce neurogenic inflammation and may, in turn, excite DRG neurons via their own receptors expressed on DRG neurons through a paracrine or an autocrine pathway (van Rossum et al., 1997; Tang et al., 2007). This study extends previous findings by providing evidence that neuronal FcγRI triggers an NSCC-TRPC3, which may contribute to the IgG-IC-induced excitation of DRG neurons.

However, these neuropathic mechanisms become critical only under certain pathological conditions. In the normal nervous system, the presence of blood-nerve/brain-barriers and glial cells protects the surface of a primary sensory neuron against large molecules such as IgG-IC and IgG. By contrast, under pathological conditions that disrupt these barriers and demyelinate the peripheral and central neurons (Abbott et al., 2003; Sastre-Garriga and Montalban, 2003; Hu and Lucchinetti, 2009), the neuronal surface is more readily exposed to IgG-IC present in the serum or surrounding tissues. Thus, IgG-IC can bind to neuronal FcγRI and directly activate the primary sensory neurons, therefore possibly inducing pain, hyperalgesia, and allodynia. However, the actual behavioral consequences of IgG-IC activation of TRPC3 channels in nociceptors remain to be determined, and nothing is known about the functions of the much more widely expressed FcγRI in the larger DRG neurons (Qu et al., 2011a) that are unlikely to be nociceptive.

In summary, this study reveals a novel mechanism whereby IgG-IC induces the activation of primary sensory neurons via the functional coupling between FcγRI and TRPC3 through the Syk–PLC–IP_3 signaling pathway. These findings might serve as a basis for the development of new therapeutic strategies for the treatment of pain related to IgG-IC-mediated immune diseases.

References

Abbott NJ, Mendonça LL, Dolman DE (2003) The blood-brain barrier in systemic lupus erythematosus. Lupus 12:908–915.

Andoh T, Kuraishi Y (2004) Direct action of immunoglobulin G on primary sensory neurons through Fc gamma receptor I. FASEB J 18:182–184.

Bonilla FA, Fujita RM, Pivniouk VI, Chan AC, Geha RS (2000) Adapter proteins SLP-76 and BLNK both are expressed by murine macrophages and are linked to signaling via Fcgamma receptors I and II/III. Proc Natl Acad Sci U S A 97:1725–1730.

Bonnington JK, McNaughton PA (2003) Signalling pathways involved in the sensitisation of mouse nociceptive neurones by nerve growth factor. J Physiol 551:433–446.

Clapham DE, Julius D, Montell C, Schultz G (2005) International Union of Pharmacology, XLIX: nomenclature and structure-function relationships of transient receptor potential channels. Pharmacol Rev 57:427–450.

Colton CK, Zhu MX (2007) 2-Aminoethoxydiphenyl borate as a common activator of TRPV1, TRPV2, and TRPV3 channels. Handb Exp Pharmacol (179):173–187.

Doerner JF, Gisselmann G, Hatt H, Wetzel CH (2007) Transient receptor potential channel A1 is directly gated by calcium ions. J Biol Chem 282:13180–13189.

Floto RA, Somasundaram B, Allen JM, Mahaut-Smith MP (1997) Fcgamma receptor I activation triggers a novel Ca2+-activated current selective for monovalent cations in the human monocytic cell line, U937. J Biol Chem 272:4753–4758.

Grynkiewicz G, Poenie M, Tsien RY (1985) A new generation of Ca2+ indicators with greatly improved fluorescence properties. J Biol Chem 260:3440–3450.

He LP, Hewavitharana T, Soboloff J, Spassova MA, Gill DL (2005) A functional link between store-operated and TRPC channels revealed by the 3,5-bis(trifluoromethyl)pyrazole derivative, BTP2. J Biol Chem 280:10997–11006.

Hofmann T, Obukhov AG, Schaefer M, Harteneck C, Gudermann T, Schultz G (1999) Direct activation of human TRPC6 and TRPC3 channels by diacylglycerol. Nature 397:259–263.

Hu HZ, Gu Q, Wang C, Colton CK, Tang J, Kinoshita-Kawada M, Lee LY, Wood JD, Zhu MX (2004) 2-aminoethoxydiphenyl borate is a common activator of TRPV1, TRPV2, and TRPV3. J Biol Chem 279:35741–35748.

Hu W, Lucchinetti CF (2009) The pathological spectrum of CNS inflammatory demyelinating diseases. Semin Immunopathol 31:439–453.

Indik ZK, Park JG, Hunter S, Schreiber AD (1995) The molecular dissection of Fc gamma receptor mediated phagocytosis. Blood 86:4389–4399.

Kaida K, Ariga T, Yu RK (2009) Antiganglioside antibodies and their pathophysiological effects on Guillain-Barre syndrome and related disorders—a review. Glycobiology 19:676–692.

Kaznacheyeva E, Glushankova L, Bugaj V, Zimina O, Skopin A, Alexeenko V, Tsiokas L, Bezprozvanny I, Mozhayeva GN (2007) Suppression of TRPC3 leads to disappearance of store-operated channels and formation of a new type of store-independent channels in A431 cells. J Biol Chem 282:23655–23662.

Kiener PA, Rankin BM, Burkhardt AL, Schieven GL, Gilliland LK, Rowley RB, Bolen JB, Ledbetter JA (1993) Cross-linking of Fc gamma receptor I (Fc gamma RI) and receptor II (Fc gamma RII) on monocytic cells activates a signal transduction pathway common to both Fc receptors that involves the stimulation of p72 Syk protein tyrosine kinase. J Biol Chem 268:24442–24448.

Kim MS, Hong JH, Li Q, Shin DM, Abramowitz J, Birnbaumer L, Muallem S (2009) Deletion of TRPC3 in mice reduces store-operated Ca2+ influx and the severity of acute pancreatitis. Gastroenterology 137:1509–1517.

Kiselyov K, Xu X, Mozhayeva G, Kuo T, Pessah I, Mignery G, Zhu X, Birnbaumer L, Muallem S (1998) Functional interaction between InsP3 receptors and store-operated Htrp3 channels. Nature 396:478–482.

Kiyonaka S, Kato K, Nishida M, Mio K, Numaga T, Sawaguchi Y, Yoshida T, Wakamori M, Mori E, Numata T, Ishii M, Takemoto H, Ojida A, Watanabe K, Uemura A, Kurose H, Morii T, Kobayashi T, Sato Y, Sato C, Hamachi I, Mori Y (2009) Selective and direct inhibition of TRPC3 channels underlies biological activities of a pyrazole compound. Proc Natl Acad Sci U S A 106:5400–5405.

Kress M, Karasek J, Ferrer-Montiel AV, Scherbakov N, Haberberger RV (2008) TRPC channels and diacylglycerol dependent calcium signaling in rat sensory neurons. Histochem Cell Biol 130:655–667.

Lai JY, Cox PJ, Patel R, Sadiq S, Aldous DJ, Thurairatnam S, Smith K, Wheeler

D, Jagpal S, Parveen S, Fenton G, Harrison TK, McCarthy C, Bamborough P (2003) Potent small molecule inhibitors of spleen tyrosine kinase (Syk). Bioorg Med Chem Lett 13:3111–3114.

Li HS, Xu XZ, Montell C (1999) Activation of a TRPC3-dependent cation current through the neurotrophin BDNF. Neuron 24:261–273.

Liao F, Shin HS, Rhee SG (1992) Tyrosine phosphorylation of phospholipase C-gamma 1 induced by cross-linking of the high-affinity or low-affinity Fc receptor for IgG in U937 cells. Proc Natl Acad Sci U S A 89:3659–3663.

Lu SG, Zhang X, Gold MS (2006) Intracellular calcium regulation among subpopulations of rat dorsal root ganglion neurons. J Physiol 577: 169–190.

Ma HT, Patterson RL, van Rossum DB, Birnbaumer L, Mikoshiba K, Gill DL (2000) Requirement of the inositol trisphosphate receptor for activation of store-operated Ca2+ channels. Science 287:1647–1651.

Ma C, Zhang P, Sikand P, LaMotte RH, Gu Q (2009) Antigen-specific immune mechanisms of chronic pain. Soc Neurosci Abstr 35:459.5.

Ma C, Greenquist KW, Lamotte RH (2006) Inflammatory mediators enhance the excitability of chronically compressed dorsal root ganglion neurons. J Neurophysiol 95:2098–2107.

Mathsson L, Lampa J, Mullazehi M, Rönnelid J (2006) Immune complexes from rheumatoid arthritis synovial fluid induce FcgammaRIIa dependent and rheumatoid factor correlated production of tumour necrosis factor-alpha by peripheral blood mononuclear cells. Arthritis Res Ther 8:R64.

McDougall JJ (2006) Arthritis and pain: neurogenic origin of joint pain. Arthritis Res Ther 8:220.

Miyano K, Morioka N, Sugimoto T, Shiraishi S, Uezono Y, Nakata Y (2010) Activation of the neurokinin-1 receptor in rat spinal astrocytes induces Ca2+ release from IP3-sensitive Ca2+ stores and extracellular Ca2+ influx through TRPC3. Neurochem Int 57:923–934.

Montell C (2008) In search of the holy grail for *Drosophila* TRP. Neuron 58:825–827.

Moulin DE (1998) Pain in central and peripheral demyelinating disorders. Neurol Clin 16:889–898.

Naraghi M (1997) T-jump study of calcium binding kinetics of calcium chelators. Cell Calcium 22:255–268.

Neher E (1998) Vesicle pools and Ca2+ microdomains: new tools for understanding their roles in neurotransmitter release. Neuron 20:389–399.

Nimmerjahn F, Ravetch JV (2006) Fcgamma receptors: old friends and new family members. Immunity 24:19–28.

Nimmerjahn F, Ravetch JV (2007) Fc-receptors as regulators of immunity. Adv Immunol 96:179–204.

Nimmerjahn F, Ravetch JV (2008) Fcgamma receptors as regulators of immune responses. Nat Rev Immunol 8:34–47.

Oaklander AL (2008) Mechanisms of pain and itch caused by herpes zoster (shingles). J Pain 9:S10–S18.

Pedersen SF, Owsianik G, Nilius B (2005) TRP channels: an overview. Cell Calcium 38:233–252.

Pinto LG, Cunha TM, Vieira SM, Lemos HP, Verri WA Jr, Cunha FQ, Ferreira SH (2010) IL-17 mediates articular hypernociception in antigen-induced arthritis in mice. Pain 148:247–256.

Poteser M, Schleifer H, Lichtenegger M, Schernthaner M, Stockner T, Kappe CO, Glasnov TN, Romanin C, Groschner K (2011) PKC-dependent coupling of calcium permeation through transient receptor potential canonical 3 (TRPC3) to calcineurin signaling in HL-1 myocytes. Proc Natl Acad Sci U S A 108:10556–10561.

Qiu J, Fang Y, Rønnekleiv OK, Kelly MJ (2010) Leptin excites proopiomelanocortin neurons via activation of TRPC channels. J Neurosci 30:1560–1565.

Qu L, Zhang P, LaMotte RH, Ma C (2011a) Neuronal Fc-gamma receptor I mediated excitatory effects of IgG immune complex on rat dorsal root ganglion neurons. Brain Behav Immun 25:1399–1407.

Qu L, Zhang P, Ma C (2011b) Activation of neuronal Fc-gamma receptor I triggers a transient receptor potential-like current in the rat dorsal root ganglion neurons. Soc Neurosci Abstr 37:380.23.

Raybould NP, Jagger DJ, Kanjhan R, Greenwood D, Laslo P, Hoya N, Soeller C, Cannell MB, Housley GD (2007) TRPC-like conductance mediates restoration of intracellular Ca2+ in cochlear outer hair cells in the guinea pig and rat. J Physiol 579:101–113.

Sanchez-Miranda E, Ibarra-Sanchez A, Gonzalez-Espinosa C (2010) Fyn kinase controls FcepsilonRI receptor-operated calcium entry necessary for full degranulation in mast cells. Biochem Biophys Res Commun 391:1714–1720.

Sastre-Garriga J, Montalban X (2003) APS and the brain. Lupus 12:877–882.

Shirakawa H, Sakimoto S, Nakao K, Sugishita A, Konno M, Iida S, Kusano A, Hashimoto E, Nakagawa T, Kaneko S (2010) Transient receptor potential canonical 3 (TRPC3) mediates thrombin-induced astrocyte activation and upregulates its own expression in cortical astrocytes. J Neurosci 30:13116–13129.

Sun JH, Yang B, Donnelly DF, Ma C, LaMotte RH (2006) MCP-1 enhances excitability of nociceptive neurons in chronically compressed dorsal root ganglia. J Neurophysiol 96:2189–2199.

Tang HB, Li YS, Arihiro K, Nakata Y (2007) Activation of the neurokinin-1 receptor by substance P triggers the release of substance P from cultured adult rat dorsal root ganglion neurons. Mol Pain 3:42.

Trebak M, Bird GS, McKay RR, Putney JW Jr (2002) Comparison of human TRPC3 channels in receptor-activated and store-operated modes: differential sensitivity to channel blockers suggests fundamental differences in channel composition. J Biol Chem 277:21617–21623.

Trebak M, Vazquez G, Bird GS, Putney JW Jr (2003a) The TRPC3/6/7 subfamily of cation channels. Cell Calcium 33:451–461.

Trebak M, St J Bird G, McKay RR, Birnbaumer L, Putney JW Jr (2003b) Signaling mechanism for receptor-activated canonical transient receptor potential 3 (TRPC3) channels. J Biol Chem 278:16244–16252.

van de Winkel JG, Tax WJ, Jacobs CW, Huizinga TW, Willems PH (1990) Cross-linking of both types of IgG Fc receptors, Fc gamma RI and Fc gamma RII, enhances intracellular free Ca2+ in the monocytic cell line U937. Scand J Immunol 31:315–325.

van Rossum D, Hanisch UK, Quirion R (1997) Neuroanatomical localization, pharmacological characterization and functions of CGRP, related peptides and their receptors. Neurosci Biobehav Rev 21:649–678.

Verri WA Jr, Cunha TM, Parada CA, Poole S, Liew FY, Ferreira SH, Cunha FQ (2007) Antigen-induced inflammatory mechanical hypernociception in mice is mediated by IL-18. Brain Behav Immun 21:535–543.

Verri WA Jr, Guerrero AT, Fukada SY, Valerio DA, Cunha TM, Xu D, Ferreira SH, Liew FY, Cunha FQ (2008) IL-33 mediates antigen-induced cutaneous and articular hypernociception in mice. Proc Natl Acad Sci U S A 105:2723–2728.

Wittkowski A, Richards HL, Griffiths CE, Main CJ (2007) Illness perception in individuals with atopic dermatitis. Psychol Health Med 12:433–444.

Wu LJ, Sweet TB, Clapham DE (2010) International Union of Basic and Clinical Pharmacology, LXXVI: current progress in the mammalian TRP ion channel family. Pharmacol Rev 62:381–404.

Xu SZ, Zeng F, Boulay G, Grimm C, Harteneck C, Beech DJ (2005) Block of TRPC5 channels by 2-aminoethoxydiphenyl borate: a differential, extracellular and voltage-dependent effect. Br J Pharmacol 145:405–414.

Zitt C, Obukhov AG, Strübing C, Zobel A, Kalkbrenner F, Lückhoff A, Schultz G (1997) Expression of TRPC3 in Chinese hamster ovary cells results in calcium-activated cation currents not related to store depletion. J Cell Biol 138:1333–1341.